

De Novo Design of an Allosteric Metalloprotein Assembly with Strained Disulfide Bonds

Lewis A. Churchfield, Annette Medina-Morales, Jeffrey D. Brodin, Alfredo Perez, and F. Akif Tezcan*

Department of Chemistry and Biochemistry, University of California, San Diego, La Jolla, California 92093-0356, United States

S Supporting Information

ABSTRACT: A major goal in metalloprotein design is to build protein scaffolds from scratch that allow precise control over metal coordination. A particular challenge in this regard is the construction of allosteric systems in which metal coordination equilibria are coupled to other chemical events that take place elsewhere in the protein scaffold. We previously developed a metal-templated self-assembly strategy (MeTIR) to build supramolecular protein complexes with tailorable interfaces from monomeric building blocks. Here, using this strategy, we have incorporated multiple disulfide bonds into the interfaces of a Zn-templated cytochrome *cb₅₆₂* assembly in order to create mechanical strain on the quaternary structural level. Structural and biophysical analyses indicate that this strain leads to an allosteric system in which Zn²⁺ binding and dissociation are remotely coupled to the formation and breakage of a disulfide bond over a distance of >14 Å. The breakage of this strained bond upon Zn²⁺ dissociation occurs in the absence of any reductants, apparently through a hydrolytic mechanism that generates a sulfenic acid/thiol pair.

In association with proteins, metal ions fulfill central biological roles that range from structural stabilization and signaling to electron transfer and catalysis.^{1,2} At the core of these diverse roles lies an exquisite interplay between the energetics of the bound metals and the protein matrix.^{3–5} This interplay is well understood at the level of the primary and secondary coordination spheres of metal ions, and has been recapitulated in biomimetic systems^{6,7} and designed or reengineered proteins.^{8,9} Considerably more difficult to model is the relationship between metal coordination/reactivity and outer-sphere interactions at the tertiary and quaternary structure level. Allostery and cooperativity are particularly striking manifestations of the control of metal coordination through outer sphere interactions, as embodied by hemoglobin and metalloregulatory proteins. In hemoglobin, structural changes that result from O₂ coordination to a single heme cofactor are propagated onto the entire quaternary architecture, causing the structural equilibrium of the protein to shift from the “tense” state to the “relaxed” state, thereby leading to progressively more favorable O₂ binding (positive cooperativity) by the remaining heme cofactors.¹⁰ Similarly, in metalloregulatory proteins, the equilibria for metal ion coordination are remotely coupled to those for DNA binding, enabling the regulation of gene transcription in response to ambient metal concentrations.¹¹

De novo construction of allosteric systems like hemoglobin and metalloregulatory proteins represents an outstanding goal in protein design. The challenge therein stems not only from the necessity to design at least two (re)active sites in a single protein, but also from the requirement to efficiently couple these sites via a structural conduit. Clearly, these design criteria (>two reactive sites and remote coupling) would disfavor scaffolds that are small or possess extreme rigidity or flexibility. In fact, a large number of natural allosteric proteins are large, oligomeric complexes that contain semirigid subunits linked by flexible interfaces.^{12–14} In this way, mechanical strain generated by a chemical event in one site can be transmitted onto the interfaces and propagated throughout the entire superstructure. Although allosteric proteins have been engineered through different strategies, these typically involve either the modification of existing proteins that undergo ligand-specific conformational changes or the fusion of protein domains with pre-existing chemical functions.^{15–18} Here, we report the de novo construction of an allosteric protein assembly with flexible interfaces, in which two distinct chemical functions, metal binding and disulfide bond formation, and the structural elements that couple these functions are designed in concert. This study highlights how quaternary strain can be built in a bottom-up fashion such that (a) the thermodynamics of metal ion coordination can be regulated through outer sphere interactions, and (b) metal binding can be remotely coupled to reversible disulfide bond formation, a premier chemical strategy that nature uses for redox regulation.^{19,20}

Our strategy for building quaternary strain is based on Metal-Templated Interface Redesign (MeTIR), an approach we developed for the construction of functional metalloprotein assemblies. Using MeTIR, we have previously reported that a monomeric protein (cytochrome *cb₅₆₂*) could be decorated with metal chelating groups, which direct the self-assembly of *cyt cb₅₆₂* into a discrete tetrameric architecture (Zn₄·MBPC1₄, abbreviated as Zn-M1₄) upon Zn²⁺ coordination (Figure S1).^{21,22} This D₂ symmetric tetramer presents three pairs of C₂ symmetric interfaces (*i1*, *i2*, and *i3*) that are independently tailorable, forming a tunable shell around the four internalized Zn²⁺ coordination sites. We first incorporated favorable, noncovalent interactions into the *i1* interfaces through six, primarily hydrophobic mutations to obtain the variant RIDC1 (hereafter referred to as R1) (Figure S1).²³ This was followed by the incorporation of disulfide linkages into the *i2* and *i3* interfaces through T96C and E81C mutations.^{24,25} The resulting tetramer

Received: August 15, 2016

Published: September 20, 2016

$C_{81}/C_{96}R_{14}$ could self-assemble efficiently from the monomeric building blocks with the proper formation of C81–C81 and C96–C96 disulfide linkages and coordinate Zn^{2+} ions with high affinity as intended by the templating strategy (Figures 1 and

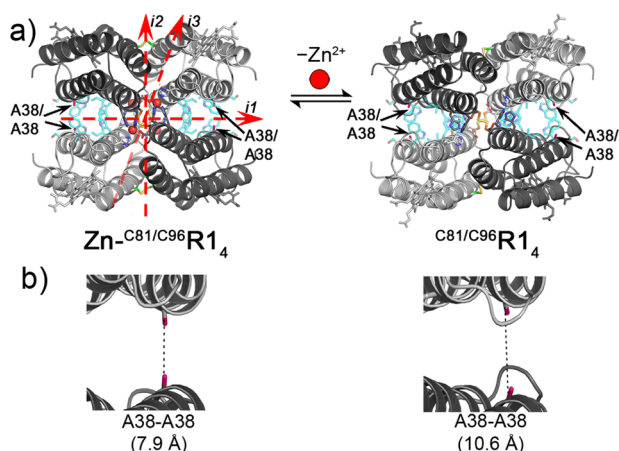


Figure 1. (a) Scheme showing structural rearrangements in the tetramer $Zn-C_{81}/C_{96}R_{14}$ upon Zn^{2+} removal (PDB IDs: 4JE9 and 4JEA). The hydrophobic residues in the $i1$ interface are shown as cyan sticks. A38-A38 residue pairs are indicated. (b) Close-up view of A38-A38 residue pairs. Dashed lines denote α -C separations.

S1).²⁵ Successive engineering of the interfaces has two consequences: first, it increases the overall rigidity and preorganization of the quaternary assembly, thus turning it increasingly more into a monolithic architecture. Second, it increases the overall strain that Zn^{2+} coordination and the interfacial interactions exert on one another. The strain is evident when comparing the structures of Zn-bound and apo- $C_{81}/C_{96}R_{14}$ (Figure 1). In particular, the hydrophobically stabilized $i1$ interfaces (side chains shown in cyan in Figure 1) undergo a substantial deformation upon Zn^{2+} removal, whereby the average α -C distance between the symmetrically related A38 residues increases from 7.9 to 10.6 Å. This deformation is accompanied by conformational changes in the C96–C96 and C81–C81 linkages that hold the $i2$ and $i3$ interfaces together in a hinge-like fashion (Figure S2). In this study, we set out to examine if the $i1$ interfaces in $C_{81}/C_{96}R_{14}$ could also be disulfide-cross-linked through the incorporation of a Cys residue at position 38. We envisioned that this would generate a spring-loaded quaternary structure with highly strained and potentially dissociable disulfide bonds that could allow structural coupling between Zn-binding and disulfide bond formation equilibria.

Toward this end, we generated the triple Cys mutant $C_{38}/C_{81}/C_{96}R_{14}$, which was expressed in *Escherichia coli* and isolated as a monomer in high yield. Given the presence of three Cys residues on the surface of $C_{38}/C_{81}/C_{96}R_{14}$, the formation of unstructured, disulfide-linked aggregates over the desired tetramer ($C_{38}/C_{81}/C_{96}R_{14}$) becomes a potential concern. Nevertheless, we found that the self-assembly of $C_{38}/C_{81}/C_{96}R_{14}$ under air oxidation preferentially gave rise to a tetrameric species in relatively high yield ($47 \pm 4\%$, Figure S3). The inclusion of 1.5-fold molar excess of Zn^{2+} ions gave a slight but reproducible increase in the yield of the tetrameric species ($53 \pm 7\%$). These observations suggest that the hydrophobic mutations engineered to stabilize the $i1$ interface likely align the $C_{38}/C_{81}/C_{96}R_{14}$ monomers in the proper orientation for the desired disulfide bonds (C38–C38, C81–C81, C96–C96 rather than any

heteropair) to form, and that Zn^{2+} ions have a modest templating effect. Indeed, oxidative self-assembly of the variant $C_{38}/C_{81}/C_{96}M1$ lacking the hydrophobic mutations led primarily to the population of higher-order aggregates (Figure S3) with no preference for the formation of the tetrameric species (16% yield).

The $C_{38}/C_{81}/C_{96}R_{14}$ tetramer, self-assembled in the presence of Zn^{2+} ions, was isolated in high purity (>90%, Figure 2a) by size-

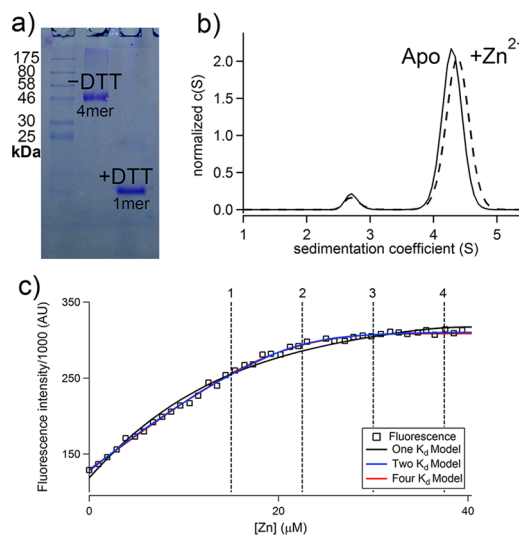


Figure 2. (a) Nonreducing SDS-PAGE of $C_{38}/C_{81}/C_{96}R_{14}$ in the absence and presence of DTT. (b) Sedimentation velocity profile of $C_{38}/C_{81}/C_{96}R_{14}$ in the presence of excess EDTA or 1 equiv of Zn^{2+} . (c) Zn-binding isotherm of $C_{38}/C_{81}/C_{96}R_{14}$ determined using Fura-2 as a competing ligand. Vertical lines indicate equivalents of Zn^{2+} added in excess of Fura-2.

exclusion chromatography and treated with EDTA to produce fully demetalated stock solutions. Upon treatment with the reducing agent dithiothreitol (DTT), $C_{38}/C_{81}/C_{96}R_{14}$ fully dissociated into a monomeric form (Figure 2a), confirming that its self-assembly is mediated by disulfide bond formation. The narrow and symmetric sedimentation-velocity profile of $C_{38}/C_{81}/C_{96}R_{14}$ ($S_{max} = 4.3$) is consistent with a closed tetrameric architecture that undergoes a slight structural rearrangement upon binding Zn^{2+} ($S_{max} = 4.4$) (Figure 2b). We examined the Zn binding properties of $C_{38}/C_{81}/C_{96}R_{14}$ using the fluorophore Fura-2, which exhibits an increase in fluorescence intensity at 335 nm upon Zn^{2+} coordination (Figure S4), as a competitive ligand for metal binding ($K_{d,Fura2-Zn} = 5.7$ nM).²⁴ The competitive binding isotherm showed the expected stoichiometry of four Zn^{2+} ions per tetramer, and could be fit by a thermodynamic model with two pairs of equivalent Zn-binding sites and two corresponding equilibrium constants ($K_d = 8.1 \pm 0.4$ and 400 ± 100 nM; overall $\Delta G_{Zn} = -164 \pm 1$ kJ/mol) (Tables 1 and S1). These values indicate a significantly diminished Zn-binding affinity for $C_{38}/C_{81}/C_{96}R_{14}$ compared to the previously characterized tetramers $C_{96}R_{14}$ ($\Delta G_{Zn} = -186 \pm 2$ kJ/mol) and $C_{81}/C_{96}R_{14}$ ($\Delta G_{Zn} = -183 \pm 1$ kJ/mol),^{24,25} which feature one and two pairs of disulfide bonds, respectively. These findings indicate that the presence of all three pairs of interfacial disulfide bonds imparts a strain at the level of the quaternary architecture, manifested in the destabilization of Zn^{2+} coordination by ~ 20 kJ/mol.

To get a deeper insight into how the interfacial disulfide linkages influence Zn-binding thermodynamics, we conducted

Table 1. Thermodynamic Parameters for Zn Binding Determined by Competitive Titrations^a and ITC

R ₁₄ variant	total ΔG_{Zn} (kJ/mol)	total ΔH_{ITC} (kJ mol ⁻¹)	total ΔS_{ITC} (kJ K ⁻¹ mol ⁻¹)
C ⁹⁶ R ₁₄	-186 ± 2 ^b	62 ± 13	0.84 ± 0.05
C ⁸¹ /C ⁹⁶ R ₁₄	-183 ± 1 ^c	59 ± 1	0.82 ± 0.01
C ³⁸ /C ⁸¹ /C ⁹⁶ R ₁₄	-164 ± 1	10 ± 0.3	0.59 ± 0.01

^aReported uncertainties correspond to fitting errors from single competitive titration measurements. Apparent Zn-binding enthalpies (ΔH_{ITC}) were determined by isothermal titration calorimetry. Reported errors are standard deviations among at least three replicate measurements. Apparent Zn-binding entropies (ΔS_{ITC}) were derived from the measured ΔG_{Zn} and ΔH_{ITC} values. ^bFrom ref 24. ^cFrom ref 25.

isothermal titration calorimetry (ITC) experiments with C⁹⁶R₁₄, C⁸¹/C⁹⁶R₁₄ and C³⁸/C⁸¹/C⁹⁶R₁₄ scaffolds, bearing one, two and three pairs of disulfide bonds, respectively. In all cases, the ITC thermograms were consistent with the coordination of four Zn²⁺ ions per tetramer (Figure S5), and allowed us to estimate the apparent Zn binding enthalpies (ΔH_{ITC}) in combination with the thermodynamic parameters derived from fluorescence titrations (Tables 1 and S1) (see Supporting Information for additional experimental details). Because the primary Zn²⁺ coordination spheres are conserved in all three tetramers (see below and Figure S6), their measured ΔH_{ITC} values can be meaningfully compared without deriving their condition-independent Zn-binding enthalpies (ΔH_{Zn}).²⁶ Our analysis reveals that C⁹⁶R₁₄ and C⁸¹/C⁹⁶R₁₄ display nearly identical ΔH_{ITC} values of 62 and 59 kJ/mol, respectively. Strikingly, Zn²⁺ coordination by C³⁸/C⁸¹/C⁹⁶R₁₄ is significantly more exothermic ($\Delta H_{\text{ITC}} = 10$ kJ/mol). This 50 kJ/mol decrease in enthalpy suggests that there may be a distinct structural change associated with the C³⁸/C⁸¹/C⁹⁶R₁₄ architecture that is coupled to Zn²⁺ coordination.²⁷

We determined the X-ray crystal structures of Zn-bound and apo-C³⁸/C⁸¹/C⁹⁶R₁₄ at 2.1 and 2.4 Å resolution, respectively (PDB IDs: 5L32 and 5L31) (Table S2). As designed, Zn-C³⁸/C⁸¹/C⁹⁶R₁₄ contains four Zn-coordination sites and is structurally very similar to its predecessors Zn-C⁹⁶R₁₄ and Zn-C⁸¹/C⁹⁶R₁₄ both in terms of overall topology (α -C RMSD = 1.78 and 1.02 Å, respectively) and primary/secondary Zn²⁺ coordination spheres (Figures 3 and S6). The presence of all planned interfacial disulfide bonds is clearly evident from the electron density maps (Figure S7). To our knowledge, the Zn-C³⁸/C⁸¹/C⁹⁶R₁₄ scaffold represents the first designed protein that self-assembles into a closed architecture through the formation of six covalent bonds. All three pairs of disulfides adopt distinct conformations in Zn-C³⁸/C⁸¹/C⁹⁶R₁₄, with the C38–C38 disulfide pairs possessing the highest strain energy as calculated using the method reported by Katz and Kossiakoff (Table S3).²⁸

Indeed, the apo-C³⁸/C⁸¹/C⁹⁶R₁₄ structure reveals that, upon removal of Zn²⁺, one of the two C38–C38 disulfide pairs is broken. This yields a tetrameric architecture that now contains five disulfide bonds and does not possess the original D₂ symmetry of the Zn-bound assembly any longer (Figure 3a–c). Despite extensive disulfide cross-linking, there is a sizable conformational shift from the Zn-bound to the apo-C³⁸/C⁸¹/C⁹⁶R₁₄ structure (RMSD = 2.55 Å) (Figure S8). This shift is paralleled by the rearrangement of all existing disulfide bonds whose calculated strain energies decrease upon Zn²⁺ removal (Table S3). These observations suggest that Zn²⁺

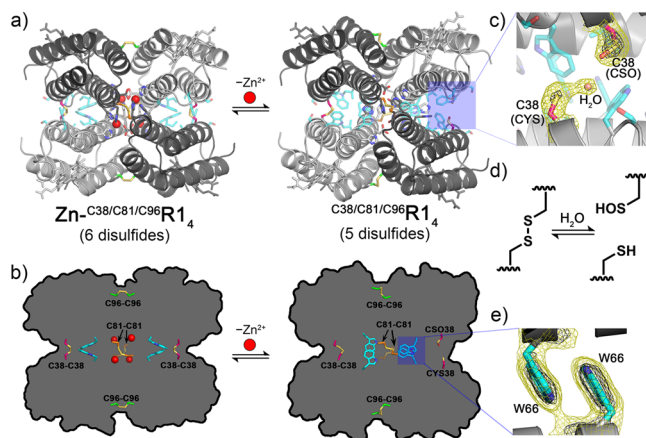


Figure 3. (a) X-ray crystal structures of Zn-C³⁸/C⁸¹/C⁹⁶R₁₄ and the metal-free C³⁸/C⁸¹/C⁹⁶R₁₄. The broken C38–C38 disulfide bond is highlighted with a blue box. Disulfide bonds, Zn-binding sites, and the engineered hydrophobic mutations in *i1* (cyan) are shown as sticks. (b) Scheme highlighting rearrangements of interfacial residues in Zn-C³⁸/C⁸¹/C⁹⁶R₁₄ upon Zn²⁺ removal. (c) Close-up view of the broken C38–C38 disulfide bond, forming a cysteine (CYS) and cysteine sulfenic acid (CSO). A water molecule H-bonded to CYS 38 is shown as a pink sphere. (d) Hydrolytic dissociation of a disulfide bond into a sulfenic acid-thiol pair. (e) Close-up view of the W66–W66 π -stacking interaction. All $2F_o - F_c$ electron density maps are contoured at 1σ (yellow) and 2.5σ (black).

coordination spring-loads the quaternary architecture through the formation of strained disulfide bonds, and that this strain is relieved through the dissociation of a single C38–C38 bond that is >14 Å away from the nearest Zn²⁺ coordination site. The fact that the Zn-C³⁸/C⁸¹/C⁹⁶R₁₄ crystals were obtained by adding Zn²⁺ to apo-C³⁸/C⁸¹/C⁹⁶R₁₄ stock solutions indicates that C38–C38 bond formation is reversible (see Supporting Information). Moreover, the direct coupling between Zn²⁺ coordination and reversible disulfide bond formation in C³⁸/C⁸¹/C⁹⁶R₁₄ is consistent with its significantly more exothermic Zn²⁺ binding enthalpy compared to C⁹⁶R₁₄ and C⁸¹/C⁹⁶R₁₄, which do not contain dissociable disulfide bonds.

The breakage of the C38–C38 linkage is accompanied by a considerable distortion of the *i1* interface, whereby the distance between the α -C's of the C38 residues increases from 5.5 to 10.6 Å. This distortion largely involves the sliding of the two protein monomers with respect to another, which is enabled by the fluidity of the hydrophobic interactions in *i1*. Notably, two sets of Trp residues (W41 and W66) that form the core of the *i1* interface adopt new arrangements in the vicinity of the cleaved C38–C38 disulfide bond. The W66 side chains are now found in a π -stacking arrangement with an interplanar distance of ~ 3 Å (in contrast to a distance of >10 Å in the Zn-C³⁸/C⁸¹/C⁹⁶R₁₄ structure), likely making a major contribution to the stability of the *i1* interface in the apo-state (Figure 3b,e).

Given that there are no reducing agents in any of the protein solutions, the question arises as to how the C38–C38 bond is broken upon Zn²⁺ dissociation. A mechanistic clue is provided by the elongated electron density associated with one of the C38 side chains (Figure 3c and Figure S9), suggesting the formation of a cysteine sulfenic acid. Although the reversible 2-electron/2-proton reduction is the most common reaction manifold for disulfide bonds, they can also undergo reversible conversion into a sulfenic acid–thiol pair through hydrolysis (Figure 3d).^{19,29} Whether through redox chemistry or hydrolysis, the reactivity of disulfides is thought to depend on mechanical strain.^{30,31}

However, based on recent work with model compounds, it has been suggested that disulfide reactivity may instead be correlated with increased solvent accessibility.³² An analysis of the relative accessible surface areas³³ of the disulfide bonds indicates that the C38–C38 disulfide bonds in Zn- and apo-C₃₈/C₈₁/C₉₆R₁₄ are the least solvent-exposed (Table S4). These data suggest that it is the quaternary strain imposed by the C₃₈/C₈₁/C₉₆R₁₄ scaffold on the C38–C38 disulfide bonds that poises one of them to undergo hydrolytic cleavage upon Zn removal.

We have reported here the de novo construction of a protein complex, C₃₈/C₈₁/C₉₆R₁₄, through a metal-templating strategy, whereby a quaternary strain was built through the formation of disulfide bonds across protein interfaces. This strain has two important consequences: first, it has enabled the modulation of metal coordination thermodynamics exclusively through outer sphere interactions and led to an “energization” of the metal ions by 20 kJ/mol. This stands in contrast to most examples in molecular design where metal coordination and reactivity are exclusively handled at the primary and secondary coordination spheres.^{6,9} Second, the increased strain has allowed metal coordination to be directly and remotely linked to the formation/breakage of a distinct disulfide bond within the quaternary scaffold, thereby creating an allosteric system. Individually, metal coordination and disulfide bond formation are commonly employed as allosteric effectors in biological systems.^{11,19,20,34} The C₃₈/C₈₁/C₉₆R₁₄ scaffold represents a unique system that links these two effectors to one another. More generally, our study illustrates the power of supramolecular protein design in creating artificial biological systems with coupled and externally controllable functions.

■ ASSOCIATED CONTENT

■ Supporting Information

The Supporting Information is available free of charge on the ACS Publications website at DOI: 10.1021/jacs.6b08458.

- Additional experimental details and data (PDF)
- Coordinate file for apo-C₃₈/C₈₁/C₉₆R₁₄ (CIF)
- Structure factor file for apo-C₃₈/C₈₁/C₉₆R₁₄ (CIF)
- Coordinate file for Zn-C₃₈/C₈₁/C₉₆R₁₄ (CIF)
- Structure factor file for Zn-C₃₈/C₈₁/C₉₆R₁₄ (CIF)

■ AUTHOR INFORMATION

Corresponding Author

*tezcan@ucsd.edu

Notes

The authors declare no competing financial interest.

■ ACKNOWLEDGMENTS

We thank D. Wilcox, C. Quinn and W. Song for numerous helpful discussions. This work was funded by the NSF (CHE1306656 and CHE1607145 to F.A.T.), by the NIH through traineeships to J.D.B, L.A.C and A.M.-M., as well as by UCSD MARC and Amgen Scholars Program scholarships to A.P. Crystallographic data were collected at SSRL, which is supported by the DOE, Office of Science, Office of Basic Energy Sciences and Biological and Environmental Research, as well as by the NIH.

■ REFERENCES

(1) Lippard, S.; Berg, J. *Principles of Bioinorganic Chemistry*; University Science Books: Mill Valley, CA, 1994.

- (2) Bertini, I.; Gray, H. B.; Stiefel, E. I.; Valentine, J. S. *Biological Inorganic Chemistry, Structure & Reactivity*; University Science Books: Sausalito, CA, 2007.
- (3) Wittung-Stafshede, P. *Acc. Chem. Res.* **2002**, *35*, 201.
- (4) Barker, P. D. *Curr. Opin. Struct. Biol.* **2003**, *13*, 490.
- (5) Song, W. J.; Sontz, P. A.; Ambroggio, X. I.; Tezcan, F. A. *Annu. Rev. Biophys.* **2014**, *43*, 409.
- (6) Cook, S. A.; Hill, E. A.; Borovik, A. S. *Biochemistry* **2015**, *54*, 4167.
- (7) Que, L.; Tolman, W. B. *Nature* **2008**, *455*, 333.
- (8) Zastrow, M. L.; Pecoraro, V. L. *Coord. Chem. Rev.* **2013**, *257*, 2565.
- (9) Lu, Y.; Yeung, N.; Sieracki, N.; Marshall, N. M. *Nature* **2009**, *460*, 855.
- (10) Yuan, Y.; Tam, M. F.; Simplaceanu, V.; Ho, C. *Chem. Rev.* **2015**, *115*, 1702.
- (11) Reyes-Caballero, H.; Campanello, G. C.; Giedroc, D. P. *Biophys. Chem.* **2011**, *156*, 103.
- (12) Cui, Q.; Karplus, M. *Protein Sci.* **2008**, *17*, 1295.
- (13) Changeux, J.-P. *Annu. Rev. Biophys.* **2012**, *41*, 103.
- (14) Goodsell, D. S.; Olson, A. J. *Annu. Rev. Biophys. Biomol. Struct.* **2000**, *29*, 105.
- (15) Raman, S.; Taylor, N.; Genuth, N.; Fields, S.; Church, G. M. *Trends Genet.* **2014**, *30*, 521.
- (16) Choi, J. H.; Laurent, A. H.; Hilser, V. J.; Ostermeier, M. *Nat. Commun.* **2015**, *6*, 6968.
- (17) Ha, J.-H.; Loh, S. N. *Chem. - Eur. J.* **2012**, *18*, 7984.
- (18) Vallée-Bélisle, A.; Plaxco, K. W. *Curr. Opin. Struct. Biol.* **2010**, *20*, 518.
- (19) Hogg, P. J. *Trends Biochem. Sci.* **2003**, *28*, 210.
- (20) Messens, J.; Collet, J. F. *Antioxid. Redox Signaling* **2013**, *18*, 1594.
- (21) Salgado, E. N.; Faraone-Mennella, J.; Tezcan, F. A. *J. Am. Chem. Soc.* **2007**, *129*, 13374.
- (22) Bailey, J. B.; Subramanian, R. H.; Churchfield, L. A.; Tezcan, F. A. *Methods Enzymol.* **2016**, *580*, 223.
- (23) Salgado, E. N.; Ambroggio, X. I.; Brodin, J. D.; Lewis, R. A.; Kuhlman, B.; Tezcan, F. A. *Proc. Natl. Acad. Sci. U. S. A.* **2010**, *107*, 1827.
- (24) Brodin, J. D.; Medina-Morales, A.; Ni, T.; Salgado, E. N.; Ambroggio, X. I.; Tezcan, F. A. *J. Am. Chem. Soc.* **2010**, *132*, 8610.
- (25) Medina-Morales, A.; Perez, A.; Brodin, J. D.; Tezcan, F. A. *J. Am. Chem. Soc.* **2013**, *135*, 12013.
- (26) Campanello, G. C.; Ma, Z.; Grosseohme, N. E.; Guerra, A. J.; Ward, B. P.; Dimarchi, R. D.; Ye, Y.; Dann, C. E.; Giedroc, D. P. *J. Mol. Biol.* **2013**, *425*, 1143.
- (27) Conversely, the C₃₈/C₈₁/C₉₆R₁₄ exhibits a less-favorable entropy gain upon Zn binding (Table 1). Though changes in entropy can arise from multiple sources, the observed trend is consistent with decreased conformational flexibility of this scaffold compared to C₉₆R₁₄ and C₈₁/C₉₆R₁₄.
- (28) Katz, B. A.; Kosiakoff, A. *J. Biol. Chem.* **1986**, *261*, 15480.
- (29) Kettenhofen, N. J.; Wood, M. J. *Chem. Res. Toxicol.* **2010**, *23*, 1633.
- (30) Vogel, V. *Annu. Rev. Biophys. Biomol. Struct.* **2006**, *35*, 459.
- (31) Dopieralski, P.; Ribas-Arino, J.; Anjukandi, P.; Krupicka, M.; Kiss, J.; Marx, D. *Nat. Chem.* **2013**, *5*, 685.
- (32) Kucharski, T. J.; Huang, Z.; Yang, Q. Z.; Tian, Y.; Rubin, N. C.; Concepcion, C. D.; Boulatov, R. *Angew. Chem., Int. Ed.* **2009**, *48*, 7040.
- (33) Ahmad, S.; Gromiha, M.; Fawareh, H.; Sarai, A. *BMC Bioinf.* **2004**, *5*, 51.
- (34) Philips, S. J.; Canalizo-Hernandez, M.; Yildirim, I.; Schatz, G. C.; Mondragon, A.; O'Halloran, T. V. *Science* **2015**, *349*, 877.